Catena 201 (2021) 105199

Contents lists available at ScienceDirect

Catena

journal homepage: www.elsevier.com/locate/catena

Assessment of climate change impacts on the streamflow for the Mun River in the Mekong Basin, Southeast Asia: Using SWAT model

Chaoyue Li, Haiyan Fang *

Key Laboratory of Water Cycle and Related Land Surface Processes, Institute of Geographic Sciences and Natural Resources Research, Chinese Academy of Sciences, Beijing 100101, China
College of Resources and Environment, University of Chinese Academy of Sciences, Beijing 100049, China

ARTICLE INFO

Keywords:
Climate change
SWAT
Streamflow
Mun River Basin
Southeast Asia

ABSTRACT

The typical warm and wet regions of Southeast Asia have significant water resource issues. Deep insight of the future streamflow in the region is therefore necessary for effective water resource management and prediction. We coupled the Soil and Water Assessment Tool (SWAT) with a downscaling method (Delta) and global circulation models (GCMs) in the Mun River Basin (MRB), in Thailand under three Representative Concentration Pathways (RCPs). The results show that the calibrated SWAT model can accurately characterize the hydrological process on the daily, monthly, and yearly terms. The future monthly minimum temperature would rise by >1.5 °C, >2 °C, and >3 °C in the 2030s, 2060s, and 2080s respectively, under all RCPs (2.6, 4.5, and 8.5), which would also occur at the maximum temperature. The temperature increase in dry season was more significant than that of the wet season. The average annual precipitation decreased in the 2030s, and increased by 8.9%, 12.8%, and 13.9% in the 2060s under the three climate scenarios, respectively. Moreover, precipitation from June to September in wet season markedly increased. The streamflow was projected to increase by 10.5%, 20.1%, and 23.2% during 2020–2093 under three climate scenarios, respectively. Monthly average streamflow increased from June to September and decreased from February to May, and the dry seasonal streamflow decreased by 1.1%-37.2%. These changes in flow were closely related to climate change. Monthly flow changes were negatively related to temperature ($p < 0.05$) in dry season and positively linked to precipitation ($p < 0.01$) in wet season. The results of this study highlight the impact of climate change on streamflow in the Southeast Asia and provide scientific basis for adaptive management.

1. Introduction

The accumulation of greenhouse gases in the atmosphere is the dominant cause of global climate change (Nijssen et al., 2001; Nilawar and Waikar, 2019). The consensus of atmospheric scientists is that global warming is happening, and temperature is expected to continue to rise (Li and Fang, 2017). According to the Fifth Assessment Report of the Intergovernmental Panel on Climate Change (IPCC), global mean surface temperature (GMST) has increased by approximately 0.85 °C over the past 130 years (1880–2012; IPCC, 2013). Based on Coupled Model Intercomparison Project 5 (CMIP5), the IPCC has defined a new Representative Concentration Pathway (RCP) for climate change projection (Bhatta et al., 2019). For CMIP5, four RCPs have been formulated, including the “high” scenario in RCP8.5 increases throughout the twenty-first century before reaching the radiative forcing level of 8.5 W m^{-2}, the intermediate scenarios (RCP4.5 and RCP6.0). In addition, there is a low scenario, RCP2.6, in which radiative forcing reaching a maximum near mid-21st century before decreasing to a level of 2.6 W m^{-2} (Taylor et al., 2012). The GMST is projected to continuously increase by 0.3 °C to 0.7 °C during 2016–2035. Specifically, the GMST is projected to increase by 1 °C and >4 °C under the low and high climate change scenarios, respectively, by the end of the 21st century. The increase in global temperature has accelerated evapotranspiration rates, which has significantly altered global precipitation patterns (Paparrizos et al., 2015; Zhang et al., 2016). In addition, the changing trend of GMST and altered rainfall regimes are likely to continue over the next century (Bajracharya et al., 2018).

Climate change (i.e., increased temperature and altered rainfall patterns) is expected to significantly impact the hydrological cycle by influencing the spatio-temporal distribution of water cycle elements,

* Corresponding author.
E-mail address: fanghy@igsnrr.ac.cn (H. Fang).

https://doi.org/10.1016/j.catena.2021.105199
Received 24 February 2020; Received in revised form 5 January 2021; Accepted 20 January 2021
Available online 9 February 2021

including precipitation, evaporation, runoff, and soil moisture; these changes are expected to further influence the redistribution of water resources (Arnell, 1999; Bolch et al., 2012; Wang et al., 2013). Accurate projections of streamflow response to climate change are necessary for the effective planning and management of water resources, including the predictions of droughts and floods and promoting sustainable agriculture (Muhammad et al., 2018). Many studies have therefore assessed the impacts of climate change on water resources (Lehner et al., 2019; Tan and Gan, 2015) and demonstrated that the streamflow of one-third of the world's 200 major rivers have undergone significant changes since the 1950s. The associated risks of climate change impacts on freshwater resources increases significantly with increasing greenhouse gas concentrations. The renewable surface and groundwater resources in many arid subtropical regions are therefore expected to decrease significantly in the 21st century. The intensity and spatial distribution of precipitation are also expected to change under a global warming of 1.5 °C and 2.0 °C, (Wang et al., 2013). The frequency of annual heavy precipitation and the risk of drought are also projected to increase globally before 2070, which will be further enhanced under a global warming of 2.0 °C (Zhang and Villarini, 2017). Moreover, Europe, the Mediterranean, the Amazon, and South Africa are at a higher risk of drought under a global warming of 2.0 °C (Lehner et al., 2017). Climate change is therefore expected to aggravates the global and regional water shortage under the global warming of 2.0 °C. Such changes in sustainable water resources would have considerable consequences for global economies as well as ecosystems (Milly et al., 2005).

Previous modelling studies have generated the climate input as a single increment of temperature and percentage change of precipitation, either by adjusting the output of the climate model (Fan and Shibata, 2015; Liu et al., 2013) or revising the observed station data (Steinschneider et al., 2015). This can minimise bias in the climate model but may not adequately explain the climate regime changes projected by climate change, such as potential changes in the frequency, intensity and seasonality of precipitation (Xu et al., 2019). Many studies have also coupled general circulation models (GCMs) with hydrological models to simulate the potential impact of climate change on streamflow (Wang et al., 2018). The GCM is a type of climate model that mathematically represents the general circulation of a planet's atmosphere or ocean, which can provide reliable information on historical, current and future climates (Zhang et al., 2016). Each GCM is developed based on its own assumptions and unique mathematical representations of physical climate system processes, thus providing different climate predictions (Her et al., 2019). Generally, an ensemble of various GCMs from different groups around the world can provide better water resource assessments compared to that of a single GCM (Pierce et al., 2009), since, in some cases, the uncertainty of climate models is greater than that of hydrological simulations (Prudhomme et al., 2003). Statistical or dynamic downscaling methods are often used to reconcile the different spatio-temporal resolutions of GCMs and hydrological models. For example, Luo et al. (2018) used the Delta method to investigate the spatio-temporal characteristics of climate change in Xinjiang during 2021–2060 based on 37 GCMs. Under different climate scenarios, climate factors—such as precipitation and temperature—are generated as input data in hydrological models to project future streamflow; that is considered one of the most reliable methods for assessing water resource changes (Bhatta et al., 2019; Tan et al., 2017b; Xu, 1999).

The Soil and Water Assessment Tool (SWAT) is a physical-based, semi-distributed, basin-scale hydrological model and is one of the most suitable applications for investigating the response of streamflow to climate change (Zhang et al., 2016). For example, Bhatta et al. (2019) assessed the climate change impact on the hydrology of the Himalayan River Basin using three different time frames, based on an ensemble of CMIP5 and four Regional Climate Models (RCMs) under the RCP4.5 and RCP8.5 scenarios in the SWAT model. Moreover, Bajracharya et al. (2018) used a10-km resolution climate dataset in the SWAT model to project basin outflows in the Kaligandaki Basin, Nepal. Gan et al. (2015) also used an ensemble of climate models in combination with a glacier-enhanced SWAT hydrologic model to assess the effect of future climate changes on the glacier and hydrology of the Naryn River Basin in Central Asia.

The Mekong River is located in a tropical region in Southeast Asia and is the tenth largest river in the world (Yang et al., 2019). The water availability in tropical region is particularly sensitive to the impacts of climate change (Shrestha et al., 2018). Moreover, Thailand is vulnerable to droughts and floods due to extreme climate change in the middle of the Indo-China Peninsula in Southeast Asia. The country suffered its most severe monsoon flood in 2011, causing the death of >800 people and adversely affected 13.6 million people, with a total economic loss of $45.8 billion (USD) (Loo et al., 2015; Tan et al., 2019). It is therefore necessary to further elucidate the climate change impacts on hydrological processes in the region, as the intensity and frequency of extreme events—such as tropical cyclones, floods and droughts—are predicted to increase (Alessandra and Raya, 2013).

The Mun River in Thailand (the largest tributary of the Mekong River) supplies approximately 2.0×10^{10} m^3 water into Mekong River each year (Li et al., 2020). Therefore, changes in the Mun River's water quantity can have vital impacts on the water resources of the middle and lower reaches of the Mekong River. The Mun River Basin (MRB) is a viral agricultural region both locally and globally, as approximately 80% of the total basin area consists of agricultural land. Rain-fed rice yields in the MRB are generally lower than the potential levels due to water shortage (Prabnakorn et al., 2018; Prabnakorn et al., 2019). Streamflow change in response to future climate change may therefore affect agricultural water demand in this area (Boonwichai et al., 2018), which would increase hydrological uncertainty and enhance the challenges faced by local water resources management. Despite the wealth of environmental studies conducted in recent decades, most investigations in this area have focused on heavy metal pollutions, water quality, and rice yield (Akter and Babel, 2012; Liang et al., 2019; Zhao et al., 2018). In comparison, seldom information was known in relation to streamflow and water resource under the future climate change. An effective assessment on streamflow is therefore crucial for sustainable agricultural development in the MRB as well as the entire Mekong River Basin.

The main objectives of this study were to assess the response of streamflow to future precipitation and temperature changes on annual, seasonal, and monthly scales. The results contribute towards the growing literature on streamflow changes under global warming over the MRB. This study also provides a scientific reference to river basin management to mitigate future water resource issues in the MRB. Moreover, the present work has major implications for water resources in the Mekong River Basin and across the Indo-China Peninsula.

2. Materials and method

2.1. Study area

The Mun River has a length of 550 km, and is one of the important tributaries of the Mekong River, Southeast Asia (Fig. 1). It originates from the Khao Yai National Park and joins the Mekong at Khong Chiam in the Ubon Ratchathani province in Thailand (Akter and Babel, 2012). The MRB covers an area of approximately 1.19×10^5 km^2, with an elevation range of 96–1339 m (average 223 m; Fig. 2a). Most of the basin consists of flat topography, with slope gradients of less than 9% (Fig. 2d).

The tropical savannah climate of the study area has distinct wet and dry seasons (Prabnakorn et al., 2018) and is dominated by the Southeastern monsoon. The rainy season occurs from May to October, while the dry season occurs from November to April. The region has a mean annual precipitation of >1000 mm, most of which occurs in the rainy season. Monthly temperature ranges from 24 °C to 30 °C, with the lowest and highest temperatures occurring in January and April, respectively.

The MRB consists of six land use types (Fig. 2b). The main land use is

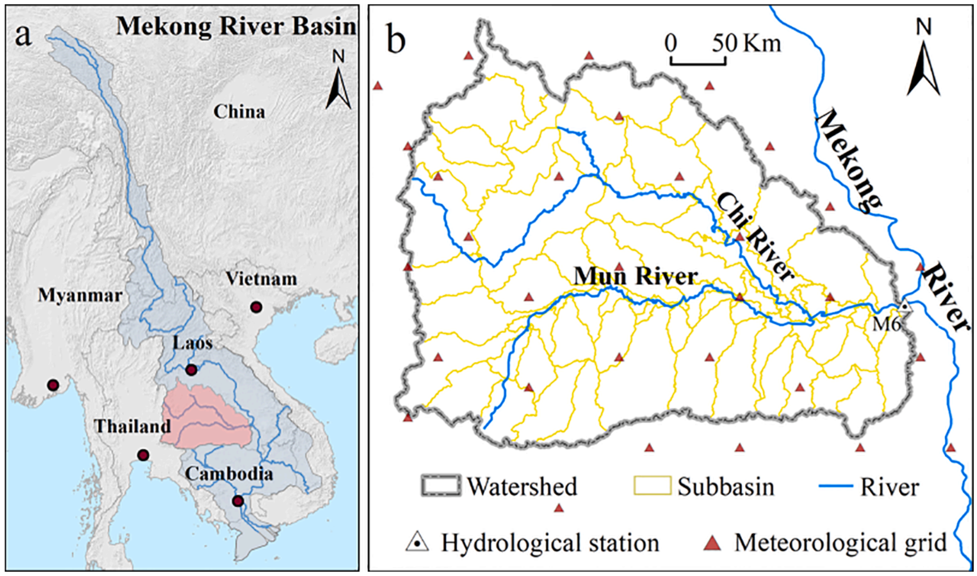

Fig. 1. Location of the study area and river monitoring network.

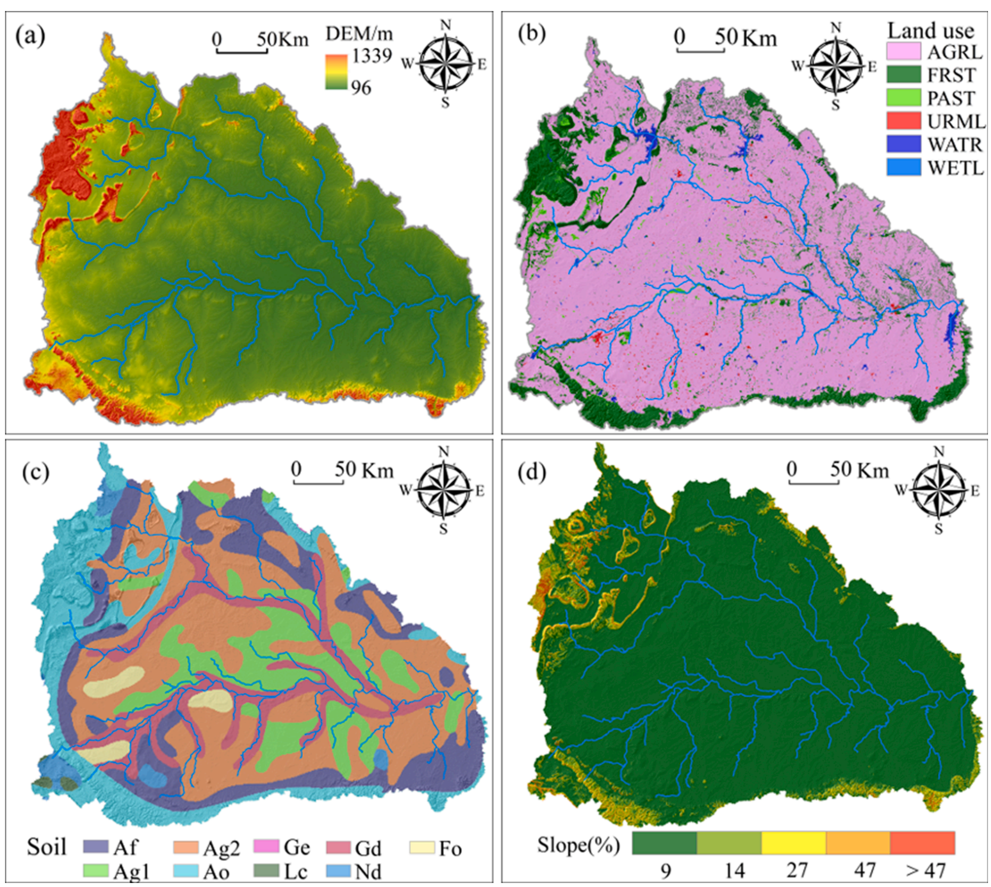

Fig. 2. Characteristics of (a) DEM, (b) land use, (c) soil, and (d) slope (AGRL, Agricultural Land; PAST, Pasture; FRST, Forest; WETL, Wetlands; WATR, Water; URML, Residential-Med/Low Density; Af, Ferric Acrisols; Ag2, Gleyic Acrisols2; Ge, Eutric Gleysols; Gd, Dystric Gleysols; Fo, Orthic Ferralsols; Ag1, Gleyic Acrisols1; Ao, Orthic Acrisols; Lc, Chromic Luvisols; Nd, Dystric Nitosols).

agriculture land (AGRL, 80% of the basin), followed by forest land (FRST, 15.04%), grass land (PAST, 2.28%), water bodies (WATR, 1.61%) and land for construction (URML, 1.10%). Rice is the main agricultural crop in the region, and forests are mainly located in the mountainous areas along the edges of the basin. Moreover, the study area has eight soil types (Fig. 2c). The Gleyic Acrisols (Ag) is the main soil type (48.82%), followed by Dystric Gleysols (Gd, 12.5%), Ferric Acrisols (Af, 17.38%), and Orthic Acrisols (Ao, 16.97%).

2.2. Data collection

2.2.1. Hydrometeorological data

Daily precipitation (Prec) data at a spatial resolution of 0.25° × 0.25° were obtained from the Asian Precipitation-High-Resolved Observational Data Integration Towards Evaluation of Water Resource (APHRODITE) (http://aphrodite.st.hirosaki-u.ac.jp/). APHRODITE is a long-term daily gridded precipitation dataset for Asia based on a dense network of rain gauges (Yatagai et al., 2012). Many studies have used APHRODITE as the ground observation data across Asian to assess its regional applicability and streamflow simulation (Chen et al., 2018; Tan et al., 2017a). Maximum temperature (T_{max}) and minimum temperature (T_{min}) data were obtained from the Global Surface Summary of the Day (GSOD) and Global Historical Climate Network Daily (GHCN) (https://www.ncdc.noaa.gov/). The bilinear interpolation method was used to interpolate the T_{max} and T_{min} to 0.25°×0.25° resolution. In this study, 31 grids of meteorological data were selected for the MRB (Fig. 1b). Based on the T_{max} and T_{min}, the Hargreaves method was used to calculate potential evapotranspiration (Pereia and Prutit, 2004).

Streamflow data at the M6 gauge station during 1980–2004 were used for model calibration (Fig. 1b). The data were obtained from the Department of Water Resources of Ministry of Natural Resources and Environment of Thailand. The average annual streamflow was 809.8 m^3 s^{-1}, and the average flow during the rainy season was 613.8 m^3 s^{-1}, accounting for approximately 75.8% of the total annual streamflow.

2.2.2. Topographic, soil, and land use data

The Digital Elevation Model (DEM) was produced by the Shuttle Radar Topography Mission (SRTM) at 30-m resolution. The DEM was provided by the Geospatial Data Cloud site from the Computer Network Information Center in the Chinese Academy of Sciences (http://www.gscloud.cn).

The Harmonized World Soil Database (HWSD) Version 1.2 was obtained from the Food and Agriculture Organization of the United Nations (FAO-UN; http://www.fao.org). Soil properties—such as soil depth, organic carbon, and sand, clay and silt percentages—were also available and can be used directly in the SWAT model. Soil characteristics, including bulk density, available water, and saturation hydraulic conductivity, were calculated using the Soil-Plant-Air-Water (SPAW) software.

As this study focused on the impact of climate change on basin streamflow, only one-phase land use in 2000 was employed. Land use was kept unchanged during the model simulation process, and land use data with a resolution of 30 m was obtained from GlobeLand30.

2.3. SWAT model

The SWAT model is a distributed watershed hydrological model (Arnold et al., 1998) developed by the Agricultural Research Service of the U.S. Department of Agriculture (USDA ERS). It can be used to simulate the quality and quantity of surface and ground water as well as their responses to land management (Olivera et al., 2006). The data required to run SWAT include rainfall and temperature, land use, soil types and properties, DEM, and hydrology. Based on these datasets, a basin is divided into multiple sub-basins and hydrologic response units (HRUs) according to the minimum threshold ratio of land use, soil type and slope (Jha, 2012). In the present study, the MRB was divided into 70 sub-basins and 1063 HRUs.

The SWAT-simulated hydrological process is divided into the hydrological cycle and the confluence phase. The hydrological cycle is based on the water balance equation (Osei et al., 2019):

$$SW_t = SW_0 + \sum_{i=1}^{t}(R_{day} - Q_{surf} - E_a - w_{seep} - Q_{gw}) \tag{1}$$

where SW_t (mm H_2O) is the final soil water content at day t, SW_0 (mm H_2O) is the initial soil water content, t(d) is time, R_{day} (mm H_2O) is the amount of precipitation at day i, Q_{surf} (mm H_2O) is the amount of surface streamflow at day i, E_a (mm H_2O) is the amount of evapotranspiration at day i, w_{seep} (mm H_2O) is the amounts of percolation and bypass flow in the soil profile bottom at day i, and Q_{gw} (mm H_2O) is the amount of return flow at day i (Nilawar and Waikar, 2019).

In SWAT, the Soil Conservation Service curve number procedure (SCS-CN) and the Green and Ampt infiltration methods are applied to estimate surface runoff. The SCS submodel was developed to provide a consistent basis for estimating the amount of runoff under various land use and soil types. The Green and Ampt equation was applied to predict infiltration assuming excess water at the surface at all times. The surface runoff can be estimated using the SCS curve equation as follows:

$$Q_{surf} = \frac{(R_{day} - I_a)^2}{(R_{day} - I_a + S)} \tag{2}$$

where, I_a (mm H_2O) is the initial abstraction, including interception, infiltration and surface storage for the day, and S (mm H_2O) is the retention parameter. The retention parameter changes spatially due to changes in soil, land use management and slope as well as temporary change in soil moisture. Parameter S is defined as:

$$S = 25.4\left(\frac{1000}{CN} - 10\right) \tag{3}$$

Table 1
Details of the 34 CMIP5 climate models.

ID	Model Name	Country	Institution	Resolution Lon × Lat
1	ACCESS1.0	Australia	CSIRO-BOM	1.88°×1.25°
2	ACCESS1.3	Australia	CSIRO-BOM	1.88°×1.25°
3	BCC-CSM1.1	China	BCC	2.81°×2.79°
4	BNU-ESM	China	GCESS	2.81°×2.79°
5	CanESM2	Canada	CCCma	2.81°×2.79°
6	CCSM4	America	NCAR	1.25°×0.94°
7	CESM1(CAM5)	America	NSF-DOE-NCAR	1.25°×0.94°
8	CESM1 (WACCM)	America	NSF-DOE-NCAR	1.25°×0.94°
9	CMCC-CMS	Italy	CMCC	1.88°×1.88°
10	CNRM-CM5	France	CNRM-CERFACS	1.41°×1.40°
11	CSIRO-Mk3.6.0	Australia	CSIRO-QCCCE	1.88°×1.88°
12	EC-EARTH	Ten European countries	EC-EARTH	1.13°×1.13°
13	FGOALS-g2	China	LASG-CESS	2.81°×2.81°
14	FIO-ESM	China	FIO	2.80°×2.80°
15	GFDL-ESM2G	America	NOAA GFDL	2.00°×2.02°
16	GFDL-ESM2M	America	NOAA GFDL	2.50°×2.02°
17	GISS-E2-H	America	NASA GISS	2.50°×2.00°
18	GISS-E2-R	America	NASA GISS	2.50°×2.00°
19	HadGEM2-AO	Korea	NIMR/KMA	1.88°×1.25°
20	HadGEM2-CC	England	MOHC	1.88°×1.25°
21	HadGEM2-ES	England	MOHC	1.88°×1.25°
22	INM-CM4	Russia	INM	2.00°×1.50°
23	IPSL-CM5A-LR	France	IPSL	3.75°×1.89°
24	IPSL-CM5A-MR	France	IPSL	2.50°×1.27°
25	IPSL-CM5B-LR	France	IPSL	3.75°×1.89°
26	MIROC4h	Japan	MIROC	0.56°×0.56°
27	MIROC5	Japan	MIROC	1.41°×1.40°
28	MIROC-ESM	Japan	MIROC	2.81°×2.79°
29	MIROC-ESM-CHEM	Japan	MIROC	2.81°×2.79°
30	MPI-ESM-LR	Germany	MPI-M	1.88°×1.87°
31	MPI-ESM-MR	Germany	MPI-M	1.88°×1.87°
32	MRI-CGCM3	Japan	MRI	1.13°×1.12°
33	NorESM1-M	Norway	NCC	2.50°×1.89°
34	GFDL-CM3	America	NOAA GFDL	2.50°×2.00°

where *CN* is the curve number for the day.

Model parameter sensitivity, calibration, and validation were conducted before projecting future climate change impacts on streamflow. The global sensitivity of streamflow parameter was determined using the Automated Latin Hypercube One-factor-At-a-Time (LH-OAT) procedure (Nilawar and Waikar, 2019). Fifteen parameters were chosen for the model calibration (Table 1). The sensitivity of the parameters was measured by considering the P-value and t-Stat (Tuo et al., 2016).

Calibration and validation processes were conducted after the sensitivity analysis. The calibration was performed using the daily data during 1978–1998, with the first two years as the warm-up period. The validation period was from 1999 to 2004. In this study, SWAT calibration and uncertainty programs (i.e., SWAT-CUP) were used to calibrate SWAT. The sequential uncertainty fitting algorithm (SUFI-2) was applied to analyse the sensitivity, calibration, validation, and uncertainty in the MRB. The correlation coefficient (R^2), the Nash-Sutcliffe (NS) efficiency coefficient, and percent bias (PBIAS) were used to check the satisfaction of the SWAT model.

The precipitation and temperature generated by the Delta method under RCP2.6, RCP4.5, and RCP8.5 were then used as inputs in the calibrated SWAT model to predict the future climate change impacts on

Table 2
The sensitive parameters for streamflow with their ranges and adopted values.

Rank	Parameter	Description	Range	Adopted value	t-Stat	P-Value
1	GW_DELAY	Groundwater delay time	30 to 450	33.74	−13.91	0.00
2	CN2	SCS runoff curve number	−0.2 to 0.2	0.04	10.04	0.00
3	RCHRG_DP	Deep aquifer percolation fraction	0 to 1	0.04	−7.40	0.00
4	ALPHA_BNK	Base flow alpha factor for bank storage	0 to 1	0.43	2.30	0.02
5	ESCO	Soil evaporation compensation factor	0.8 to 1	0.81	−2.27	0.02
6	CH_K2	Effective hydraulic conductivity in the main channel	5 to 130	48.53	−1.86	0.06
7	CANMX	Maximum canopy storage	0 to 100	97.74	1.60	0.11
8	REVAPMN	Threshold depth of water in the shallow aquifer for “revap” to occur	0 to 10	3.28	0.86	0.39
9	SOL_K	Saturated hydraulic conductivity	−0.8 to 0.8	0.65	−0.85	0.39
10	GWQMN	Threshold depth of water in shallow aquifer for return flow to occur	0 to 2	1.78	0.80	0.42
11	SOL_BD	Moist bulk density of first soil layer	−0.5 to 0.6	−0.24	0.44	0.66
12	GW_REVAP	Groundwater revap. coefficient	0 to 0.2	0.07	0.34	0.74
13	CH_N2	Manning’s n value for main channel	0 to 0.3	0.30	0.28	0.78
14	ALPHA_BF	Base flow alpha factor	0 to 1	0.11	0.24	0.81
15	SOL_AWC	soil available water storage capacity	−0.2 to 0.4	0.37	0.12	0.90

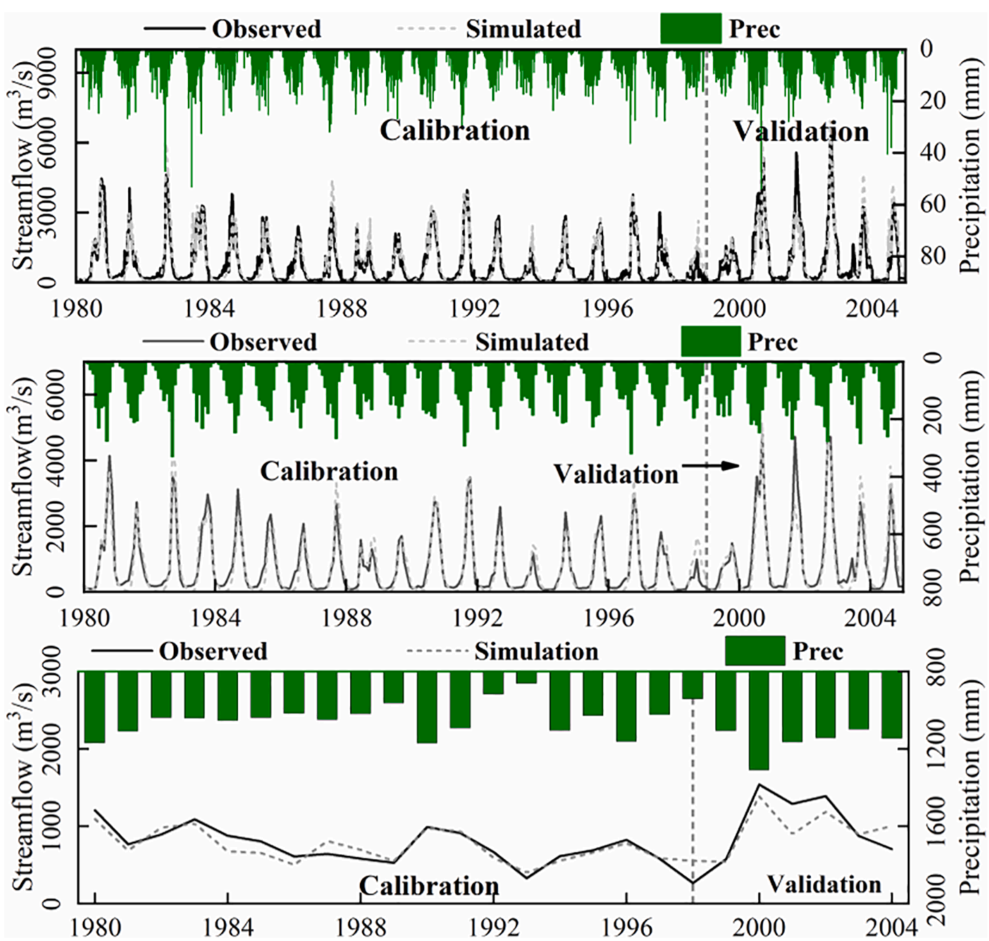

Fig. 3. Comparisons between observed and simulated streamflow at station M6 on the daily (upper), monthly (middle), and yearly (lower) time steps for calibration and validation.

streamflow.

2.4. Future climate change projection

Precipitation and temperature are the two main climatic factors affecting streamflow on the basin scale (Wang et al., 2018). Thirty-four CMIP5 GCMs were employed in this study (Table 1) and are described in detail by Ruan et al. (2018, 2019). The future climate data was also corrected by the Delta method for 2006–2093 under RCP2.6, RCP4.5, and RCP8.5. The Delta method is a relatively simple but commonly applied downscaling technique; it can also cluster the entire range of various models and calculate their average level. The major steps of the method include the following: 1) comparing the future annual precipitation of each GCM output grid with the reference period and then calculating the change proportions of precipitation, and 2) multiply the proportions by the observed precipitation of the base period to obtain the future precipitation at each station (Hay et al., 2000). It is worth noting that the Delta changes for precipitation and temperature differ: the grid variable change output by the GCM refers to the relative change for precipitation and absolute change for temperature.

The mean multi-model ensemble projected changes in precipitation and temperature for the 2030s (2020–2044), the 2060s (2045–2069), and the 2080s (2070–2093) under RCP2.6, RCP4.5, and RCP8.5, which were compared to their counterparts during baseline period (1980–2004). Each period covered a 25-year time period, and the ensemble of absolute change was calculated using the simple arithmetic mean method.

3. Results

3.1. Parameter sensitivity, calibration, and validation

Fifteen parameters were chosen for the calibration of the model are listed in Table 2. The sensitivity of the parameters was measured by considering the P-value and t-Stat (Tuo et al., 2016). The most sensitive parameters were groundwater delay (GW_DELAY), followed by the SCS runoff curve number (CN2), deep aquifer percolation fraction (RCHRG_DP), base flow alpha factor for bank storage (ALPHA_BNK), and soil evaporation compensation factor (ESCO). Generally, the most sensitive parameters were groundwater-related parameters (GW_DELAY, RCHRG_DP) and the surface runoff parameter (CN2), which is consistent with the results of previous studies (Ligaray et al., 2016; Shrestha et al., 2018).

During the calibration period, the simulated daily, monthly, and yearly streamflow values were matched with the observed values (Fig. 3). The R^2 values were 0.87, 0.90, and 0.76, and the NS values were 0.86, 0.89, and 0.76, respectively (Table 3). PBIAS values were −1.37%, −1.44%, and −1.10%, suggesting that the simulated values were generally lower than the observed values. The R^2 and NS during the validation period were 0.86, 0.89, and 0.66, and 0.85, 0.88, and 0.61, respectively. The PBIAS values were −7.54%, −7.56%, and −7.29%, and the R^2 and NS values during this period were slightly lower than those during the calibration period.

3.2. Projected changes in precipitation and temperature

3.2.1. Precipitation

The monthly precipitation in January, May, August, and December was projected to increase under all three emission scenarios and in all time frames (Fig. 4). Under the three climate scenarios, precipitation was projected to decrease in February, April, July, and November during the 2030s, and projected to increase during the 2060s and 2080s. Precipitation in March was projected to decrease during the 2060s under RCP2.6 and increase in all three time slices under RCP4.5 and RCP8.5. In June, rainfall was projected to decrease during the 2030s and the 2080s and increase during the 2060s under all three RCPs. Under RCP2.6,

Table 3
Statistical performance for the calibration and validation periods.

Objective Function	Equation*	Daily		Monthly		Yearly		Performance Rating			
		P1	P2	P1	P2	P1	P2	Very Good	Good	Satisfactory	Unsatisfactory
PBIAS (%)	$PBIAS = 100\cdot\left[\frac{\sum_{i=1}^{n} Q'_i - Q_i}{\sum_{i=1}^{n} Q_i}\right]$	−1.37	−7.54	−1.44	−7.56	−1.09	−7.29	PBIAS<±10	±10 ≤ PBIAS≤±15	±15 ≤ PBIAS≤±25	PBIAS ≥ 25
R^2	$R^2 = \frac{\left[\sum_{i=1}^{n}\left(Q_i-\overline{Q}_i\right)\left(Q'_i-\overline{Q}'_i\right)\right]^2}{\sum_{i=1}^{n}\left(Q_i-\overline{Q}_i\right)^2\sum_{i=1}^{n}\left(Q'_i-\overline{Q}'_i\right)^2}$	0.87	0.86	0.90	0.89	0.76	0.66	$0.75 < R^2 \le 1$	$0.65 < R2 \le 0.75$	$0.5 < R^2 \le 0.65$	$R^2 \le 0.5$
NS	$NS = 1 - \frac{\sum_{i=1}^{n}\left(Q_i - Q'_i\right)^2}{\sum_{i=1}^{n}\left(Q_i - \overline{Q}_i\right)^2}$	0.86	0.85	0.89	0.88	0.76	0.61	$0.75 < NS \le 1$	$0.65 < NS \le 0.75$	$0.5 < NS \le 0.65$	$NS \le 0.5$

*R: Correlation coefficient between simulated and observed data; Q_i and Q'_i: observed and simulated data, respectively; $\overline{Q}_i$ and $\overline{Q}'_i$: mean observed and simulated data, respectively.
n: total number of observations; P1: calibration (1980–1998), P2: validation (1999–2004).

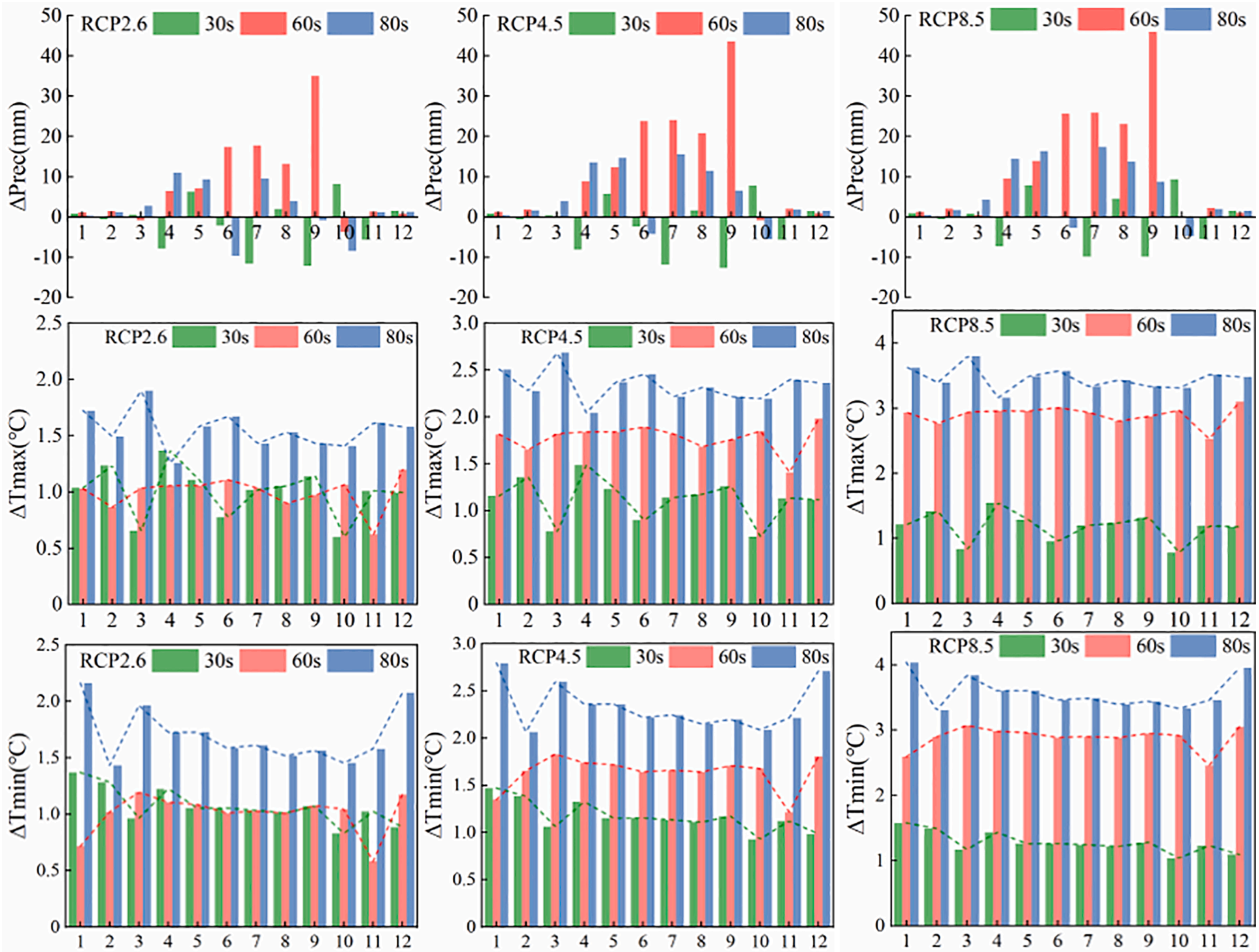

Fig. 4. Ensemble of absolute changes in monthly precipitation (Prec, upper), minimum temperature (T_{min}, middle), and maximum temperature (T_{max}, lower) in the 2030s, 2060s, and 2080s in reference to the baseline (1980–2004).

September precipitation was projected to decrease during the 2030s and the 2080s and increase (35.04 mm) during the 2060s. Moreover, October precipitation was projected to decrease in the 2060s and the 2080s and increase in the 2030s.

Precipitation in the rainy season was projected to increase during the 2060s and the 2080s under all scenarios, while a decrease was predicted for the 2030s under RCP2.6 and RCP4.5 (Fig. 5a). During the 2060s, the absolute changes of precipitation in wet season were projected to be 87 mm, 124 mm, and 135 mm under RCP2.6, RCP4.5 and RCP8.5, respectively. The dry season precipitation was projected to consistently increase during the 2060s and 2080s under the three scenarios, but was projected to decrease by 9.1%, 9.5%, and 8.1% under all three scenarios during the 2030s.

3.2.2. Temperature

Both the mean T_{min} and T_{max} were projected to increase under all RCP scenarios throughout the 21st century (Fig. 4). The absolute T_{min} changes in January, March, April, May, and December were higher than those in other months—except for the 2060s. Under RCP2.6, the average increase in monthly T_{min} were expected to range from 0.8 °C to 1.4 °C in the 2030s, 0.6 °C to 1.2 °C in the 2060s, and 1.4 ℃ to 2.2 °C in the 2080s. Under RCP4.5, the increase in monthly T_{min} was projected to range from 0.9 °C to 1.5 °C in the 2030s, 1.2 °C to 1.8 °C in the 2060s, and 2.1 °C to 2.8 °C in the 2080s. Similar monthly T_{min} changes were observed under the RCP8.5, ranging from 1.0 °C to 1.6 °C in the 2030s, 2.5 °C to 3.1 °C in the 2060s, and 3.3 °C to 4.0 °C in the 2080s. Notably, we observed no significant difference in monthly T_{max} or T_{min} between the different scenarios. The monthly mean T_{max} under RCP2.6 was projected to increase by 1.0 °C, 1.0 °C, and 1.5 °C in the 2030s, 2060s, 2080s, respectively. Under RCP4.5, the temperatures were projected to increase by 1.1 °C, 1.8 °C, and 2.3 °C in the 2030s, 2060s, 2080s, respectively. Finally, under RCP8.5, the monthly T_{max} was projected to increase by 0.8 °C to 1.6 °C in the 2030s, 2.5 °C to 3.1 °C in the 2060s, and 3.2 °C to 3.8 °C in the 2080s.

The projected seasonal changes in T_{min} and T_{max} are shown in Fig. 5. Seasonal T_{min} and T_{max} increased in both the wet and dry seasons across the year. A higher absolute increment for both seasons was projected for the 2080s. On average, the projected dry season temperature changes were higher than the wet season temperature changes. Notably, the projected T_{min} increment rates were generally higher than those of the T_{max}.

3.3. Climate change impact on streamflow

Streamflow was projected to change under all three scenarios in response to future climate change. The annual streamflow was projected to decrease during 2020–2093 under the RCP2.6 scenario, and a significant correlation ($R^2 = 0.83$) was observed between streamflow and precipitation (Fig. 6). In contrast, streamflow was projected to increase during 2020–2093 under the RCP4.5 and RCP8.5 scenarios, with a high positive correlation between streamflow and precipitation (determinant coefficient of 0.84). Compared to that of the baseline period, climate

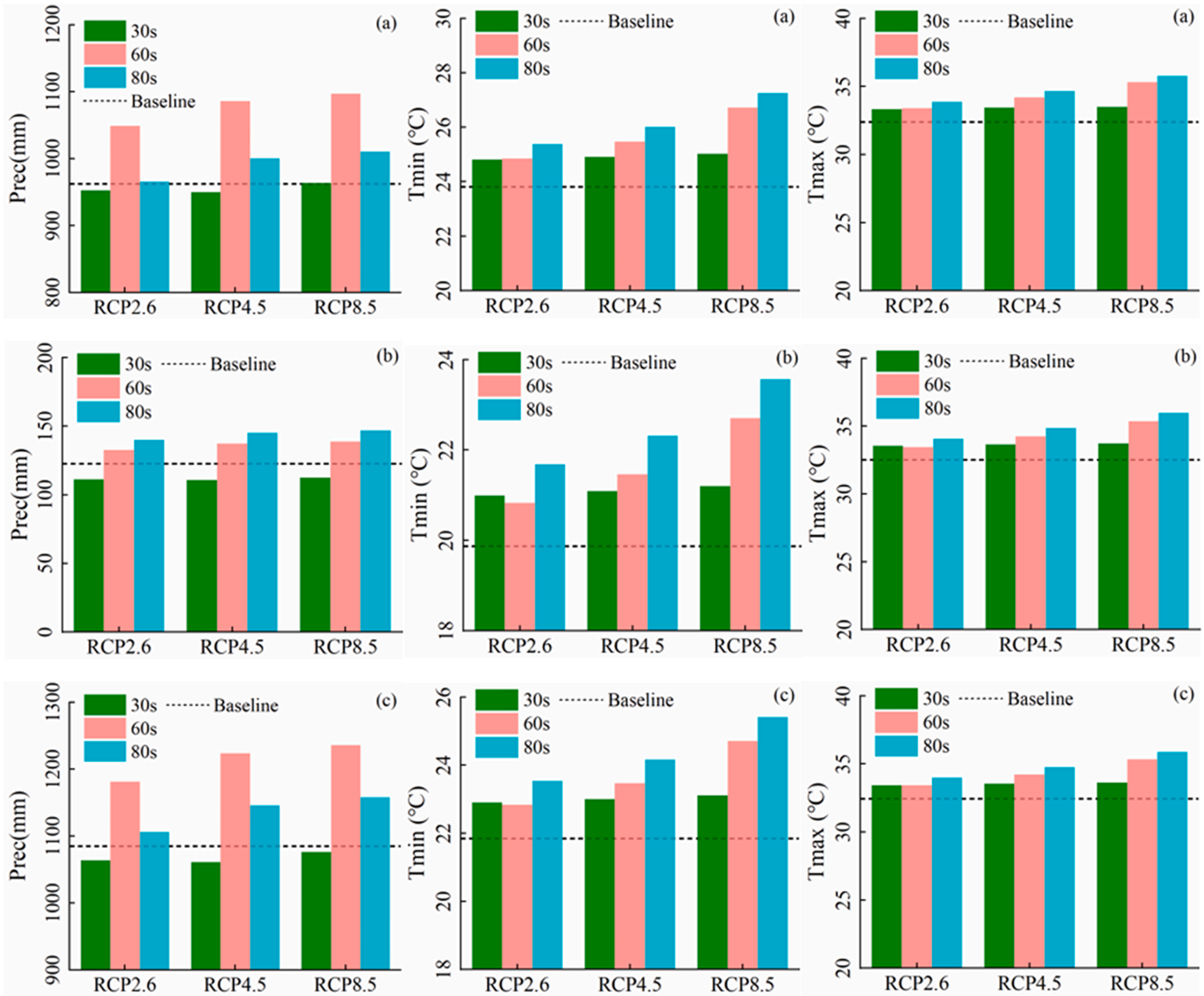

Fig. 5. Basin-wide mean changes in wet season (a), dry season (b), and annual (c) in Prec, T_{max}, and T_{min} in the 2030s, 2060s, and 2080s under three concentration scenarios.

change under the RCP8.5 scenario induced the largest increase in streamflow of 23.2% from 2020 to 2093. In contrast, streamflow under the RCP2.6 scenario showed the smallest increase from 809.3 $m^3 s^{-1}$ in the baseline period to 894.6 $m^3 s^{-1}$ (rate of increase of only 10.5%).

The changes in annual, wet, and dry season streamflow for the three future periods under RCP2.6, RCP4.5, and RCP8.5 are presented in Fig. 7. Under RCP2.6, RCP4.5, and RCP8.5, the annual streamflow decreased by 14.1%, 11.1%, and 7.6%, respectively, during the 2030s and increased by 26.0%, 40.9%, and 43.3% during the 2060s (Fig. 7a). Streamflow was projected to increase by 3.1% and 5.3% in the 2080s under the RCP4.5 and RCP8.5 scenarios, but did not increase under RCP2.6. The sensitivity of streamflow to climate change was significantly different between the dry and wet seasons. Under the three scenarios, wet season streamflow was expected to decrease in the 2030s, 2080s (Fig. 7b). However, during the 2060s, the streamflow was projected to increase by 30.1%, 45.7%, and 48.9% under RCP2.6, RCP4.5, and RCP8.5, respectively. Notably, the streamflow in the dry season was projected to decrease in all future decades under all three RCP scenarios—especially at the end of the century (Fig. 7c).

The changes in mean monthly streamflow for the entire study period (2020–2093) and the three future decades (i.e., 2030s, 2060s, and 2080s) under all scenarios are shown in Fig. 8. Although we observed the differences between each scenario throughout the study period, streamflow was generally projected to increase in January, July, August, September, and October—with a particularly significant increase in January. In contrast, streamflow was projected to decrease in February, March, April, May, November, and December—with a particularly significant decrease in April. The streamflow changes in different months under the three RCPs showed large variability for the 2030s, 2060s, and 2080s. We observed a decreasing trend in flow in most months during the 2030s. Moreover, the streamflow was projected to decrease from February to July and from October to December, with a maximum flow decrease in May. In contrast, streamflow was projected to increase in January, August, and September under the three scenarios. Compared to the streamflow in the baseline period, streamflow increased from June to November but decreased from December to May (excluding January). Moreover, the streamflow for March, April, and May was projected to significantly decrease in the 2060s. Under the RCP 2.6, RCP4.5 and RCP8.5 scenarios, streamflow was projected to decrease in the 2080s by 48.9%, 41.5%, and 41.4% in February; 75.5%, 71.2%, and 71.5% in March; 88.8%, 87.5%, and 88.4% in April; and 81.2%, 74.1%, and 66.7% in May, respectively. Notably, the decreases in streamflow exceeded 20% in November and December.

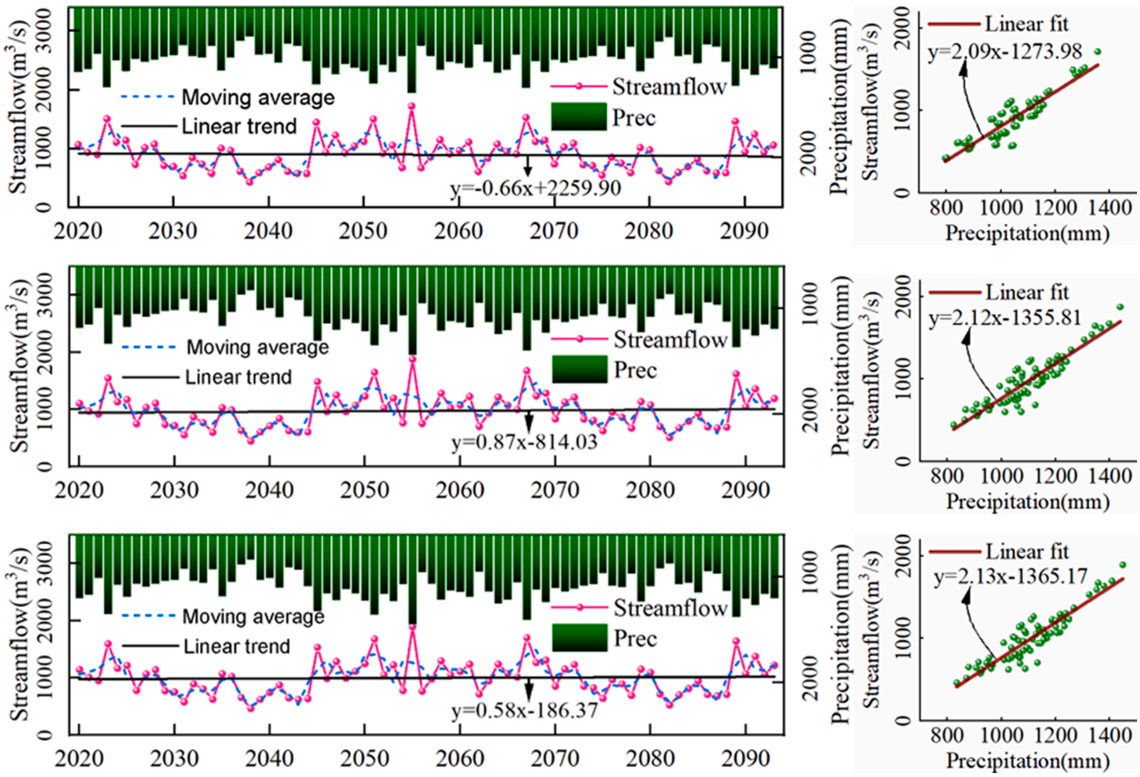

Fig. 6. The annual streamflow simulated by the calibrated SWAT model and the relations between precipitation and streamflow for 2020–2093 under the RCP2.6 (upper), RCP4.5 (middle), and RCP8.5 (lower) scenarios.

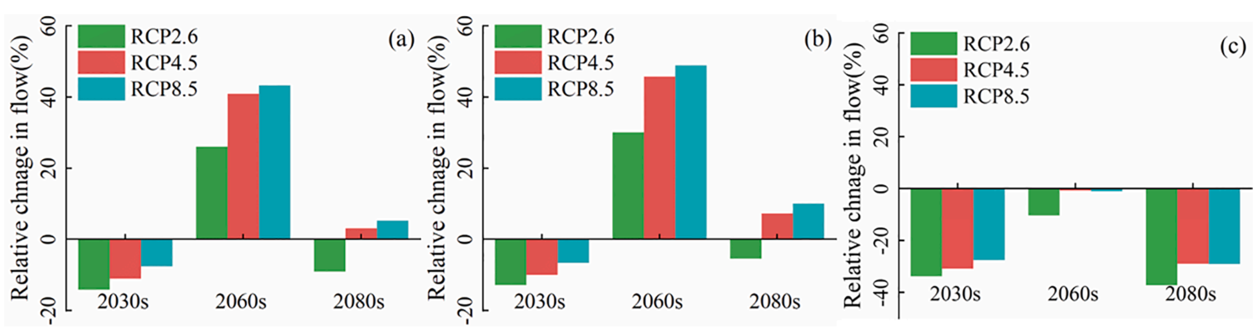

Fig. 7. Changes in mean annual (a), wet season (b), and dry season (c) streamflow for the 2030s, 2060s, and 2080s.

4. Discussion

4.1. Model performance

In this study, we employed an integrated SWAT and Delta model to project future streamflow under three climate scenarios using CMIP5 GCMs across the MRB. As this study is the first to apply the SWAT model in the MRB, we systematically evaluated its performance and applicability by comparing our results with those of other similar studies in Southeast Asia. The impact of climate change on streamflow has been successfully evaluated in the Bangpakong River Basin (Sangmanee et al., 2013), Thachin River Basin (Yasin and Clemente, 2014), and Chao Phraya River Basin (Ligaray et al., 2015) in Thailand. Generally, the model performance was between satisfactory and very good in terms of calibration and verification. The model simulated results are credible When the R^2 and NS are>0.6 and 0.5, and the PBIAS is less than 25% (Abou Rafee et al., 2019; Wang et al., 2018). In this study, the R^2, NS, and PBIAS for streamflow simulation were very good for both calibration and validation periods at different time steps (Table 2). However, it was difficult to obtain a strong fit, as hydrological processes are more complex and runoff changes more dramatic on the yearly scale. Overall, the performance of the SWAT model in this study was considered acceptable for the agricultural area of the MRB.

4.2. Precipitation and temperature change

Precipitation variability affects hydrology and streamflow (Choi et al., 2016; Fu et al., 2011). Ligaray et al. (2015) and Kure and Tebakari (2012) found that climate change increased rainfall and subsequently streamflow in the Chao Phraya Basin in Thailand. In this study, streamflow generally increased with increasing precipitation, and streamflow was mostly sensitive to the changes in annual precipitation (Table 4). A 1% increase in precipitation resulted in a streamflow increase of 3.36%, 2. 28% and 2.34% under RCP2.6, RCP4.5, and RCP8.5, respectively, which is consistent with previously published results. For example, Chiew et al. (2006) reported 1%-3% change in mean annual streamflow for every 1% change in mean annual rainfall. On the monthly scale, both the precipitation and streamflow in September

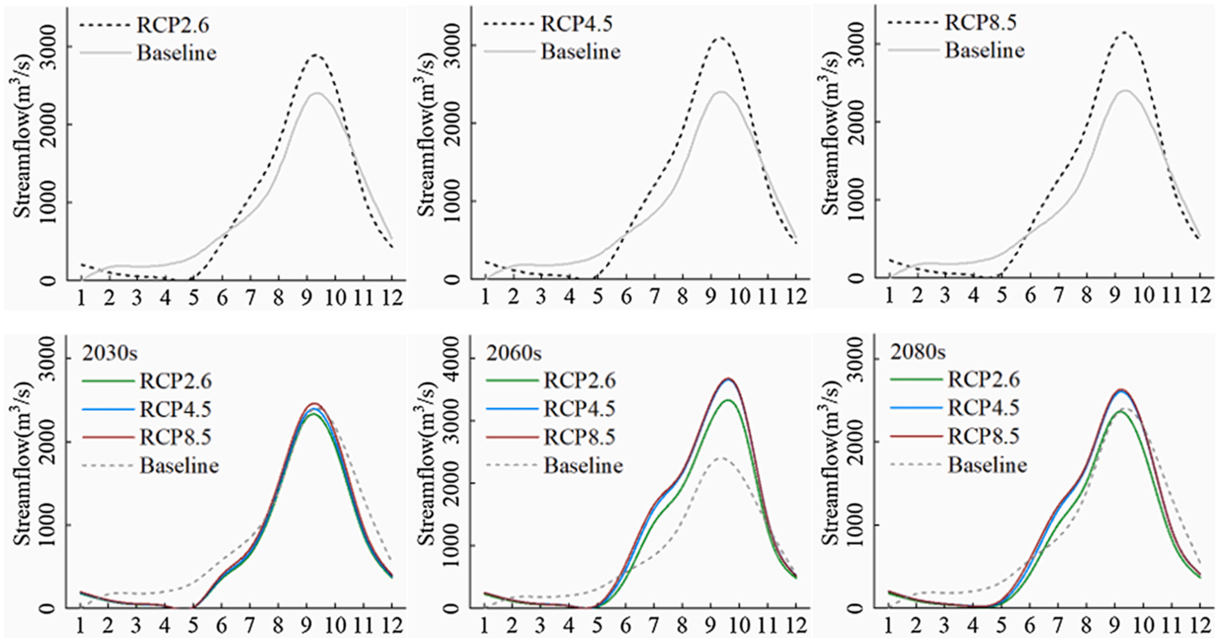

Fig. 8. Comparisons of the monthly mean streamflow between baseline and future projected period for the entire projection period (upper) and the three future decades (lower).

Table 4
Annual precipitation, temperature, and streamflow for the baseline period and the three RCP scenarios.

State variable	Baseline	RCP2.6	RCP4.5	RCP8.5
Precipitation (mm year^{-1})	1007.6	1039.1	1096.4	1107.3
Minimum yearly rainfall (mm)	794.9	795.6	823.7	835.1
Maximum yearly rainfall (mm)	1269.7	1355.8	1438.4	1447.7
Daily rainfall ≥ 10 mm per year (%)	7.55	8.13	8.46	8.65
Minimum daily temperature (°C)	21.9	23.0	23.4	24.2
Maximum daily temperature (°C)	32.6	33.6	34.1	34.8
Streamflow (m^3 s^{-1})	809.8	894.6	972.5	997.6

showed the highest increase under the RCP2.6, RCP4.5, and RCP8.5 scenarios (Figs. 4 and 8). Moreover, the dry season precipitation had increased, but the dry season flow had decreased in all three future decades (Figs. 5b and 7c), which was closely related to the observed increase in dry season temperature.

The projected temperature increases in this study are in agreement with the literature (Aggarwal et al., 2010; Arunrat et al., 2018; Furuya and Koyama, 2005) and may be responsible for the lower flows from November to April under the three scenarios (Figs. 4 and 8). The significant increase in temperature and insignificant increase in rainfall will likely accelerated water evaporation and thus decreases streamflow. The rate of temperature increase in the dry season was projected to be higher than that in the wet season, which is consistent with the findings of other studies in Thailand (Shrestha et al., 2018; Shrestha et al., 2017). Under all three scenarios, the decreased streamflow during the 2030s may due to the projected higher temperature and low rainfall –similar to the 2080s condition under the RCP2.6. In contrast, under a warmer future climate (RCP8.5 scenario), higher evaporation is unlikely to offset the negative impacts of enhanced rainfall, resulting in the higher streamflow in the 2060s (Fig. 7a and b).

4.3. Identification of the main factors

A stepwise multiple linear regression analysis inferred that the impact of annual precipitation on streamflow exceeded that of temperature in both the base period and future scenarios. However, the influencing factors varied on the monthly scale. The streamflow from May to September was mainly influenced by precipitation under the RCP2.6 and RCP4.5 scenarios. Under the RCP8.5 scenario, streamflow from May to September and November was also primarily linked to precipitation (Table 5). However, precipitation was not the only influencing factor in some months. Under the RCP2.6 scenario, the influence of precipitation and temperature was significant in April and November, and the streamflow from January to March was mostly linked to T_{max} and T_{min}. For RCP4.5, the flow in November was mainly related to precipitation and temperature, while the flow from January to March was linked to T_{max} and T_{min}. For the RCP8.5 scenario, the flow in January and March was mainly related to T_{max} and T_{min}. Under future climate change, temperature is projected to play a stronger role than precipitation during the dry season, which is similar to the findings observed in northeastern China and other regions (Li and Fang, 2017). T_{max} and T_{min} were significantly negatively correlation with streamflow during the dry season. This suggests that an increase in temperature will likely accelerate evaporation, which will exceed the impacts of precipitation and subsequently reduce streamflow (Bhatta et al., 2019). In contrast, higher rainfall was projected to occur in the wet season, which would exceed the impact of temperature and subsequently increase streamflow.

4.4. Uncertainty analysis

Future climate projections via the CMIP5 GCMs are largely uncertain (Knutti and Sedlacek, 2013). Thailand and Vietnam are the two countries with the highest number of SWAT studies in the Mekong basin. Khoi and Suetsugi (2014) reported that climate change will reduce streamflow by 0.7%-6.9% in the Be River Catchment in Vietnam. In contrast, Le and Sharif (2015) identified an increase in summer and fall river discharge during the 21st century under scenarios A2 and B1 in central Vietnam. Compared to the reference period (2003–2011), streamflow was projected to increase by 6.8%, 41.9%, and 38.4% under scenarios B1, A1B, and A2, respectively, in the Chao Phraya River Basin in Thailand (Ligaray et al., 2015), which is similar in amplitude to the streamflow changes in this study. Moreover, streamflow was projected to decrease in the Songkhram River Basin (northeast Thailand) by 19.5% and 24% under RCP4.5 and RCP8.5, respectively. These uncertainties in

Table 5
The standardized coefficients for the climate variables vs. streamflow according to the stepwise regression analysis.

	Variable	Streamflow											
		Annual	Jan	Feb	Mar	Apr	May	Jun	Jul	Aug	Sep	Oct	Nov	Dec
Baseline	Prec	0.884**					0.599**	0.883**	0.781**	0.704**	0.910**	0.540**	0.591**	
	T_{max}		−0.402*											
	T_{min}													
RCP2.6	Prec	0.973**				−0.337**	0.707**	0.658**	0.538**	0.494**	0.727**		0.313**	
	T_{max}	0.265**	−0.320*	−0.296*									−0.309**	
	T_{min}	−0.191**			−0.321**	−0.248*								
RCP4.5	Prec	0.897**					0.726**	0.654**	0.549**	0.493**	0.734**		0.339**	
	T_{max}		−0.273*										−0.236*	
	T_{min}			−0.258*	−0.289*									
RCP8.5	Prec	0.917**					0.744**	0.663**	0.556**	0.491**	0.733**		0.356**	
	T_{max}		−0.229*											
	T_{min}				−0.247*									

*Significant at the 0.05 level.
**Highly significant at the 0.01 level.

projected streamflow may be due to a number of factors, including the selected climate models, the choice of downscaling methods, the hydrological model structure, and the water conservancy measures implemented in the basins.

The primary uncertainties are related to the projections of precipitation and temperature, which impact basin hydrology and water resources (Ahmadalipour et al., 2017; Minville et al., 2008; Ouyang et al., 2015). We applied the multi-model ensemble of GCM in the present study to project future climate. We also utilised the Delta downscaling method, which can account for changes in the median of the multiple models (Luo et al., 2018). This method can also cluster the entire range of various models and calculate their average level. The disturbance factor obtained from the GCM operation is more representative and reasonable than the absolute value; this avoids the noise impact from massive datasets and filters out the overall trend (Onyutha et al., 2016). To further reduce the uncertainties of projected temperature and precipitation, an improved score-based method can be used to rank the performance of the 34 CMIP5 GCMs. Thus, appropriate models and statistical methods should be developed to quantify the impact of natural climate change and anthropogenic activities on streamflow. These aspects are beyond the scope of this study and therefore require further research.

Human activities, such as dam constructions, reservoir operations, and urban expansion, are also expected to change in response to ongoing economic development. These changes in land use have a significant impact on runoff generation and water resources (Zhou et al., 2015). In the present study, we isolated the impacts of climate change by assuming no changes in land use or other human activities. Therefore, our results can still provide a reference for future climate change impacts on streamflow.

5. Conclusions

In this study, we projected the impacts of 21st century climate change on streamflow in the MRB in Thailand, and assessed the changes in streamflow in response to three climate scenarios. The major findings of this study are summarized as follows:

(1) Compared to the baseline period (1980–2004), Tmin and Tmax are projected to increase consistently in three future time slices (2030s, 2060s, and 2080s) under three RCPs (2.6, 4.5, and 8.5). The rate of increase in the dry season temperature was greater than that in the wet season.
(2) The annual, wet season, and dry season precipitation over the MRB is projected to increase in the 2060s and 2080s under all three RCPs (2.6, 4.5, and 8.5), but decrease in the 2030s under all three climate scenarios.
(3) The streamflow in the MRB was projected to increase by 10.5%–23.2% during 2020–2093 in response to precipitation variability and temperature increase. The dry season streamflow was projected to significantly decrease by 1.1%–37.2%.
(4) The elasticity of streamflow to climate variables was not time-invariant. Precipitation was the dominant variable affecting the hydrological response on the annual scale. Moreover, temperature played a more important role during the dry season, while precipitation was more significant during the wet season. These results are crucial for the development and implementation of an effective water resource management plan in the MRB and similar basins.

Declaration of Competing Interest

The authors declare that they have no known competing financial interests or personal relationships that could have appeared to influence the work reported in this paper.

Acknowledgments

This work was supported by the Strategic Priority Research Program of Chinese Academy of Sciences A (XDA20060402) and the National Science Foundation of China (41977066). We also thank Prof. Heqing Huang and Dr. Renzhi Li for their support of the data.

References

Abou Rafee, S.A., Uvo, C.B., Martins, J.A., Domingues, L.M., Rudke, A.P., Fujita, T., Freitas, E.D., 2019. Large-Scale Hydrological Modelling of the Upper Parana River Basin. Water 11 (5).
Aggarwal, P.K., Kumar, N.S., Pathak, D.S., 2010. Impacts of climate change on growth and yield of rice and wheat in Upper Ganga Basin. WWF Report 1–44.
Ahmadalipour, A., Moradkhani, H., Rana, A., 2017. Accounting for downscaling and model uncertainty in fine-resolution seasonal climate projections over the Columbia River Basin. Clim. Dynam. 50 (1–2), 717–733.
Akter, A., Babel, M.S., 2012. Hydrological modeling of the Mun River basin in Thailand. J. Hydrol. 452, 232–246.
Alessandra, G., Raya, M., 2013. Impacts of the 2010 Droughts and Floods on Community Welfare in Rural Thailand: Differential Effects of Village Educational Attainment. Ecol. Soc. 18 (4).
Arnell, N.W., 1999. Climate change and global water resources. Global Environ. Chang. 9 (S1), S31–S49.
Arnold, J.G., Srinivasan, R., Muttiah, R.S., Williams, J.R., 1998. Large area hydrologic modeling and assessment Part I: Model Development. J. Am. Water Resour. As. 34 (1), 73–89.
Arunrat, N., Pumijumnong, N., Hatano, R., 2018. Predicting local-scale impact of climate change on rice yield and soil organic carbon sequestration: A case study in Roi Et Province, Northeast Thailand. Agr. Syst. 164, 58–70.
Bajracharya, A.R., Bajracharya, S.R., Shrestha, A.B., Maharjan, S.B., 2018. Climate change impact assessment on the hydrological regime of the Kaligandaki Basin, Nepal. Sci. Total Environ. 625, 837–848.
Bhatta, B., Shrestha, S., Shrestha, P., Talchabhadel, R., 2019. Evaluation and application of a SWAT model to assess the climate change impact on the hydrology of the Himalayan River Basin. Catena. 181.
Bolch, T., Kulkarni, A., Kabb, A., 2012. The State and Fate of Himalayan Glaciers. Science 336 (6079), 310–314.
Boonwichai, S., Shrestha, S., Babel, M.S., Weesakul, S., Datta, A., 2018. Climate change impacts on irrigation water requirement, crop water productivity and rice yield in the Songkhram River Basin, Thailand. J. Clean. Prod. 198, 1157–1164.
Chen, A.F., Chen, D.L., Azorin-Molina, C., 2018. Assessing reliability of precipitation data over the Mekong River Basin: A comparison of ground-based, satellite, and reanalysis datasets. Int. J. Climatol. 38 (11), 4314–4334.
Chiew, F.H.S., Peel, M.C., McMahon, T.A., Siriwardena, L.W., 2006. Precipitation elasticity of streamflow in catchments across the world. Climate Variability and Change - Hydrological Impacts. IAHS Publ. 308, 256.
Choi, W., Nauth, K., Choi, J., Becker, S., 2016. Urbanization and Rainfall-Runoff Relationships in the Milwaukee River Basin. Prof. Geogr. 68 (1), 14–25. https://doi.org/10.1080/00330124.2015.1007427.
Fan, M., Shibata, H., 2015. Simulation of watershed hydrology and stream water quality under land use and climate change scenarios in Teshio River watershed, northern Japan. Ecol. Indic. 50, 79–89.
Fu, G.B., Chiew, F.H.S., Charles, S.P., Mpelasoka, F., 2011. Assessing precipitation elasticity of streamflow based on the strength of the precipitation-streamflow relationship. In: 19th International Congress on Modelling and Simulation, pp. 3567–3572.
Furuya, J., Koyama, O., 2005. Impacts of Climatic Change on World Agricultural Product Markets: Estimation of Macro Yield Functions. Jarq-Jpn. Agr. Res. Q. 39 (2), 121–134.
Gan, R., Luo, Y., Zuo, Q., Sun, L., 2015. Effects of projected climate change on the glacier and runoff generation in the Naryn River Basin, Central Asia. J. Hydrol. 523, 240–251.
Hay, L.E., Wilby, R.J.L., Leavesley, G.H., 2000. A comparison of delta change and downscaled GCM scenarios for three mountainous basins in the United States. J. Am. Water Resour. Assoc. 36 (2), 387–397.
Her, Y., et al., 2019. Uncertainty in hydrological analysis of climate change: multi-parameter vs. multi-GCM ensemble predictions. Sci. Rep. 9, 22.
IPCC, 2013. In Climate Change 2013: the physical science basis contribution of Working Group I to the Fifth Assessment Report of the Intergovernmental Panel on Climate Change. Cambridge University Press, Cambridge, United Kingdom and New York, USA.
Jha, M., 2012. SWAT: Model use, calibration, and validation. T. Asabe. 55 (4), 1491–1508.
Khoi, D.N., Suetsugi, T., 2014. The responses of hydrological processes and sediment yield to land-use and climate change in the Be River Catchment, Vietnam. Hydrol. Process. 28 (3), 640–652.
Knutti, R., Sedlacek, J., 2013. Robustness and uncertainties in the new CMIP5 climate model projections. Nat. Clim. Change. 3 (4), 369–373.
Kure, S., Tebakari, T., 2012. Hydrological impact of regional climate change in the Chao Phraya River Basin, Thailand. Hydro. Res. Lett. 6, 53–58.
Le, T.B., Sharif, H.O., 2015. Modeling the Projected Changes of River Flow in Central Vietnam under Different Climate Change Scenarios. Water 7 (7), 3579–3598.
Lehner, F., et al., 2017. Projected drought risk in 1.5°C and 2°C warmer climates. Geophys. Res. Lett. 44 (14), 7419–7428.
Lehner, F., et al., 2019. The potential to reduce uncertainty in regional runoff projections from climate models. Nat. Clim. Change. 9 (12), 926–933.
Li, R.Z., et al., 2020. Trends of Runoff Variation and Effects of Main Causal Factors in Mun River, Thailand During 1980–2018. Water 12, 16.
Li, Z., Fang, H., 2017. Modeling the impact of climate change on watershed discharge and sediment yield in the black soil region, northeastern China. Geomorphology 293, 255–271.
Liang, et al., 2019. Spatial and Temporal Variation of Dissolved Heavy Metals in the Mun River, Northeast Thailand. Water 11 (2).
Ligaray, M., et al., 2015. Assessment on Hydrologic Response by Climate Change in the Chao Phraya River Basin, Thailand. Water 7 (12), 6892–6909.
Ligaray, M., Kim, H., Sthiannopkao, S., Lee, S., Kim, J.H., 2016. Assessment on Hydrologic Response by Climate Change in the Chao Phraya River Basin, Thailand. Water 7 (12), 6892–6909.
Liu, T., Merrill, N.H., Gold, A.J., Kellogg, D.Q., Uchida, E., 2013. Modeling the Production of Multiple Ecosystem Services from Agricultural and Forest Landscapes in Rhode Island. Agr. Resour. Econ. 42 (1), 251–274.
Loo, Y.Y., Billa, L., Singh, A., 2015. Effect of climate change on seasonal monsoon in Asia and its impact on the variability of monsoon rainfall in Southeast Asia. Geosci. Front. 6 (6), 817–823.
Luo, M., et al., 2018. Defining spatiotemporal characteristics of climate change trends from downscaled GCMs ensembles: how climate change reacts in Xinjiang, China. Int. J. Climatol. 38 (5), 2538–2553.
Milly, P.C.D., Dunne, K.A., Vecchia, A.V., 2005. Global pattern of trends in streamflow and water availability in a changing climate. Nature 438 (7066), 347–350.
Minville, M., Brissette, F.o., Leconte, R., 2008. Uncertainty of the impact of climate change on the hydrology of a nordic watershed. J. Hydrol. 358 (1–2), 70–83.
Muhammad, A., Uzair, Q.M., Christian, H., Ejaz, H., 2018. Future climate and cryosphere impacts on the hydrology of a scarcely gauged catchment on the Jhelum river basin, Northern Pakistan. Sci. Total Environ. 639, 961–976.
Nijssen, B., O'Donnell, G.M., Hamlet, A.F., Lettenmaier, D.P., 2001. Hydrologic Sensitivity of Global Rivers to Climate Change. Clim. Change. 50 (1–2), 143–175.
Nilawar, A.P., Waikar, M.L., 2019. Impacts of climate change on streamflow and sediment concentration under RCP 4.5 and 8.5: A case study in Purna river basin, India. Sci. Total Environ. 650, 2685–2696.
Olivera, F., Valenzuela, M., Srinivasan, R., Choi, J., Agrawal, A., 2006. ArcGIS-SWAT: A Geodata Model and GIS Interface for SWAT. J. Am. Water Resour. As. 42 (2), 295–309.
Onyutha, C., Tabari, H., Rutkowska, A., Nyeko-Ogiramoi, P., Willems, P., 2016. Comparison of different statistical downscaling methods for climate change rainfall projections over the Lake Victoria basin considering CMIP3 and CMIP5. J. Hydro-Environ. Res. 12, 31–45.
Osei, M.A., et al., 2019. The impact of climate and land-use changes on the hydrological processes of Owabi catchment from SWAT analysis. J. Hydrol. Reg. Stud. 25.
Ouyang, F., et al., 2015. Impacts of climate change under CMIP5 RCP scenarios on streamflow in the Huangnizhuang catchment. Stoch. Env. Res. Risk. A. 29 (7), 1781–1795.
Paparrizos, S., Maris, F., Matzarakis, A., 2015. Integrated analysis of present and future response of precipitation over selected Greek areas with different climate conditions. Atmos. Res. 169, 199–208.
Pereia, A.R., Prutit, W.O., 2004. Adaptation of the Thornthwaite scheme for estimating daily reference evapotranspiration. Agr. Water Manage. 66 (3), 251–257.
Pierce, D.W., Barnett, T.P., Santer, B.D., Gleckler, P.J., 2009. Selecting global climate models for regional climate change studies. P. Natl. Acad. Sci. USA 106 (21), 8441–8446.
Prabnakorn, S., Maskey, S., Suryadi, F.X., de Fraiture, C., 2018. Rice yield in response to climate trends and drought index in the Mun River Basin, Thailand. Sci. Total Environ. 621, 108–119.
Prabnakorn, S., Maskey, S., Suryadi, F.X., de Fraiture, C., 2019. Assessment of drought hazard, exposure, vulnerability, and risk for rice cultivation in the Mun River Basin in Thailand. Nat. Hazards. 97 (2), 891–911.
Prudhomme, C., Jakob, D., Svensson, C., 2003. Uncertainty and climate change impact on the flood regime of small UK catchments. J. Hydrol. 277 (1–2), 1–23.
Ruan, Y., Liu, Z., Wang, R., Yao, Z., 2019. Assessing the Performance of CMIP5 GCMs for Projection of Future Temperature Change over the Lower Mekong Basin. Atmosphere 10 (2).
Ruan, Y., Yao, Z., Wang, R., Liu, Z., 2018. Ranking of CMIP5 GCM Skills in Simulating Observed Precipitation over the Lower Mekong Basin, Using an Improved Score-Based Method. Water 10 (12).
Sangmanee, C., Wattayakorn, G., Sojisuporn, P., 2013. Simulating changes in discharge and suspended sediment loads of the Bangpakong River, Thailand, driven by future climate change. Maejo Int. J. Sci. Technol. 7, 72–84.
Shrestha, S., Bhatta, B., Shrestha, M., Shrestha, P.K., 2018. Integrated assessment of the climate and landuse change impact on hydrology and water quality in the Songkhram River Basin, Thailand. Sci. Total Environ. 643, 1610–1622.
Shrestha, S., Chapagain, R., Babel, M.S., 2017. Quantifying the impact of climate change on crop yield and water footprint of rice in the Nam Oon Irrigation Project, Thailand. Sci. Total Environ. 599, 689–699.
Steinschneider, S., Wi, S., Brown, C., 2015. The integrated effects of climate and hydrologic uncertainty on future flood risk assessments. Hydrol. Process. 29 (12), 2823–2839.
Tan, M.L., Gassman, P., Srinivasan, Arnold, J., Yang, 2019. A Review of SWAT Studies in Southeast Asia: applications, challenges and future directions. Water 11 (5).

Tan, M.L., Gassman, P.W., Cracknell, A.P., 2017a. Assessment of Three Long-Term Gridded Climate Products for Hydro-Climatic Simulations in Tropical River Basins. Water. 9 (3).

Tan, M.L., Ibrahim, A.L., Yusop, Z., Chua, V.P., Chan, N.W., 2017b. Climate change impacts under CMIP5 RCP scenarios on water resources of the Kelantan River Basin, Malaysia. Atmos. Res. 189, 1–10.

Tan, X.Z., Gan, T.Y., 2015. Contribution of human and climate change impacts to changes in streamflow of Canada. Sci. Rep. 5.

Taylor, K.E., Stouffer, R.J., Meehl, G.A., 2012. AN overview of CMIP5 and the experiment design. Bull. Amer. Meteorol. Soc. 93 (4), 485–498.

Tuo, Y., Duan, Z., Disse, M., Chiogna, G., 2016. Evaluation of precipitation input for SWAT modeling in Alpine catchment: A case study in the Adige river basin (Italy). Sci. Total Environ. 573, 66–82.

Wang, G.Q., et al., 2013. Simulating the Impact of Climate Change on Runoff in a Typical River Catchment of the Loess Plateau, China. J. Hydrometeorol. 14 (5), 1553–1561.

Wang, Y., Bian, J., Zhao, Y., Tang, J., Jia, Z., 2018. Assessment of future climate change impacts on nonpoint source pollution in snowmelt period for a cold area using SWAT. Sci Rep. 8.

Xu, C.Y., 1999. Climate Change and Hydrologic Models: A Review of Existing Gaps and Recent Research Developments. Water Resour. Manag. 13 (5), 369–382.

Xu, X., et al., 2019. Evaluating the impact of climate change on fluvial flood risk in a mixed-use watershed. Environ. Modell. Softw. 122.

Yang, J., Yang, Y.C.E., Chang, J., Zhang, J., Yao, J., 2019. Impact of dam development and climate change on hydroecological conditions and natural hazard risk in the Mekong River Basin. J. Hydrol. 579.

Yasin, H.Q., Clemente, R.S., 2014. Application of SWAT Model for Hydrologic and Water Quality Modeling in Thachin River Basin, Thailand. Arab. J. Sci. Eng. 39 (3), 1671–1684.

Yatagai, A., et al., 2012. APHRODITE: Constructing a Long-Term Daily Gridded Precipitation Dataset for Asia Based on a Dense Network of Rain Gauges. B. Am. Meteorol. Soc. 93 (9), 1401–1415.

Zhang, W., Villarini, G., 2017. Heavy precipitation is highly sensitive to the magnitude of future warming. Clim. Change. 145 (1–2), 249–257.

Zhang, Y.Q., You, Q.L., Chen, C.C., Ge, J., 2016. Impacts of climate change on streamflows under RCP scenarios: A case study in Xin River Basin, China. Atmos. Res. 178, 521–534.

Zhao, Z., Liu, G., Liu, Q., Huang, C., Li, H., 2018. Studies on the Spatiotemporal Variability of River Water Quality and Its Relationships with Soil and Precipitation: A Case Study of the Mun River Basin in Thailand. Int. J. Env. Res. Pub. He. 15 (11).

Zhou, J., et al., 2015. Integrated SWAT model and statistical downscaling for estimating streamflow response to climate change in the Lake Dianchi watershed, China. Stoch. Env. Res. Risk A. 29 (4), 1193–1210.